Quantifying the Effect of Canopy Architecture on Optical Measurements of Leaf Area Index Using Two Gap Size Analysis Methods

Jing M. Chen and Josef Cihlar, *Senior Member, IEEE*

Abstract— **In recent years, the methodology in ground-based optical measurements of leaf area index (LAI) of plant canopies has been substantially improved after the introduction of canopy gap size analysis methods. In this paper, the two methods by Chen and Black [9] and Chen and Cihlar [10] are compared for four boreal conifer stands located near Prince Albert, Saskachewan, and Thompson, Manitoba, Canada. The data used in the analysis were obtained from a new sunfleck-LAI instrument, the TRAC (Tracing Radiation and Achitecture of Canopies), which measures the photosynthetic photon flux density along transects beneath the overstory at a rate of 100 samples per meter. It is confirmed in this study that the needle shoots of conifer trees can be treated as the basic foliage units (elements) for radiation interception considerations. The effect of foliage clumping at scales larger than the shoots is quantified using an element clumping index. This is necessary for indirect measurements of LAI based on the gap fraction principle using optical instruments such as the LI-COR LAI-2000. The values of element clumping index derived from these two methods agree within 17% for all stands investigated. However, the values obtained using Chen and Black's method are consistently smaller than those calculated using Chen and Cihlar's method. The difference results from a negative bias introduced in the method of Chen and Black which requires the assumption for a random spatial distribution of foliage clumps (tree crowns). The method of Chen and Cihlar makes no assumption of foliage distribution patterns and is therefore more reliable. Yet, Chen and Black's method allows the derivation of several canopy architectural parameters which are useful for modeling radiative regimes in forest canopies. It is concluded that for remote sensing and other studies, a large quantity of ground truth LAI data can be acquired quickly and accurately using a combination of indirect optical measurements by the LAI-2000 for the foliage angular distribution and the TRAC for the foliage spatial distribution.**

I. Introduction

In the past decade, much attention has been given to indirect measurements of leaf area index (LAI) of plant canopies using ground-based optical instruments [1]. In many previous remote sensing studies [2]–[5], LAI values of forest stands derived using satellite spectral data were compared with those estimated using allometric relationships based on sapwood area or the tree trunk diameter at breast height. Since allometric relationships are stand-specific, much field work is required to establish a relationship for a forest stand. In recent studies [6], optical instruments were used for measuring LAI of forest stands. Although indirect measurements of LAI using optical instruments have the advantage of convenience and low labour costs, many researchers have been deterred by the drawbacks of the indirect methods. The difficulties arise from the complexity of radiation transfer in forest canopies. The major problems include 1) the unknown foliage angle distribution, 2) the error due to nonrandom foliage spatial distributions, and 3) the contribution of the supporting woody material to the radiation interception. With the available technology, we can overcome all these difficulties. Problems 1 and 2 are addressed here. Problem 3 is less serious because the contribution of woody material to radiation interception is generally small. In some cases, the contribution can be important, but it is not addressed in this paper.

When the foliage angle distribution is unknown, measurements of radiation transmittance through a plant canopy at multiple incidence angles are required to calculate LAI. The multiangular measurements can be made using optical sensors at different times of the day. The LAI-2000 Plant Canopy Analyzer (PCA) (LI-COR, Lincoln, NE) measures the transmittance of diffuse blue light from the sky through the canopy at five zenith angles. Thus the difficulty due to the unknown foliage angle distribution can be resolved. However, precautions must be taken in using the PCA transmittance measurements which may suffer from an error up to 10% or more due to the scattering of blue light in the canopy. This error is inevitable even under overcast conditions or near dawn or dusk when the direct sunlight is avoided [7].

The effect of foliage spatial distribution on light transmission through plant canopies, especially conifers, has been the major difficulty in obtaining accurate measurements of LAI using optical instruments. Conifer needles are grouped closely in shoots which themselves are confined to branches and tree crowns. Clumping of foliage increases radiation transmission through conifer canopies and, hence, reduces the LAI inverted from the measured transmittance. The effect of needle clumping in shoots can be found from measuring the ratio of half the total needle area in a shoot to the shoot intercepting area [8]. Reference [9] (hereinafter referred to as CB92) and [10] (hereinafter referred to as CC9x) developed methods for evaluating the effect of foliage clumping at scales larger than the shoot by utilizing the canopy gap size information. The effect is quantified using an element (shoot) clumping index. CB92 measured direct light transmitted through a Douglas-

Manuscript received May 24, 1994; revised September 6, 1994. This work was supported by the Canada Centre for Remote Sensing (CCRS) under a Research Grant.

The authors are with the Canada Center for Remote Sensing, Ottawa, ON, Canada K1A 0Y7.

IEEE Log Number 9409912.

fir canopy at a rate of 1 sample per 12 mm on a tramway beneath the canopy. From the measurements, a canopy gap size distribution was obtained, and the element clumping index was calculated from the distribution assuming that the foliage elements are randomly distributed within each foliage clump (tree crown) and that the clumps are randomly distributed in space. These assumptions are reasonably good for natural forests but not for plantations where trees are artificially spaced. CC9x developed a new gap size analysis method which avoids making these assumptions and, in theory, can be applied to all plant canopies including natural forests, plantations, as well as heterogeneous and sparse vegetation covers. They developed a new sunfleck-LAI instrument, named the TRAC (Tracing Radiation and Architecture of Canopies), which measures transmitted direct light along straight transects beneath the canopy. The instrument and the associated algorithms have been successfully tested in two conifer plantations by CC9x.

In our effort to develop algorithms for deriving LAI from remotely sensed vegetation indices as part of the BOREAS (Boreal Ecosystem and Atmosphere Study), we acquired data using the TRAC at four conifer tower flux sites in Saskachewan and Manitoba, Canada. The purpose of this paper is 1) to evaluate the advantages and disadvantages of the gap size analysis methods of CB92 and CC9x, and 2) to compare the element clumping index values derived from the two methods. It will be shown that canopy gap size information can be used to eliminate the impact of nonrandom foliage spatial distribution on indirect LAI measurements. As a result, the indirect measurements of LAI using optical sensors can be more accurate than partial direct measurements through destructive sampling.

II. Theory

The probability $P(\theta)$ of a beam or ray of light penetrating a canopy without being intercepted at an incidence angle θ is given by [11]

$$P(\theta) = \exp[-G(\theta)\Omega L/\cos\theta] \tag{1}$$

where $G(\theta)$ is the mean projection of unit leaf area on the plane perpendicular to the beam direction, being 0.5 for a spherical distribution of the normal to the leaves; L is the leaf area index defined as half the total leaf area per unit ground surface area [12]; and Ω is a dispersion parameter depending on the spatial distribution pattern of the foliage, being unity if the leaves are randomly distributed in space. Plant canopies, especially forest stands, are generally clumped, resulting in more radiation penetration through the canopy than the random case with the same L and hence Ω values smaller than unity. Ω is, therefore, more often called the clumping index [7]. Optical instruments such as the LAI-2000 PCA measure $P(\theta)$. To obtain L from $P(\theta)$ using [1], it is required to know Ω. Otherwise, only the product of Ω and L can be obtained, which is termed "the effective LAI" [7].

Foliage clumping occurs at several scales. In conifer forests, leaves (needles) are grouped in shoots, shoots are distributed within branches, and branches are organized within tree crowns. Since shoots of conifer trees appear to be distinct units of foliage, they have been treated as the foliage elements [8]–[10], [13]–[15], and (1) can be rewritten as [10]

$$P(\theta) = \exp[-G_E(\theta)\Omega_E L_E/\cos\theta] \tag{2}$$

where all terms with the subscript E have the same definitions as the corresponding terms in (1) except that they are for elements other than leaves. Here, L_E is defined as half the total element area per unit ground surface layer. The total element area is an imaginary area enveloping the element. If the area of a shoot projected onto a plane perpendicular to the direction of projection does not vary with the angular position of the shoot, i.e., the projected area can be approximated with a sphere [10], the total element area is four times the projected area because the total sphere area is four times the projected area of the sphere. If clumping occurs only at the shoot scale, i.e., shoots are randomly distributed in the whole canopy, then the element clumping index Ω_E equals unity. In reality, because shoots are grouped in branches and tree crowns, foliage clumping at scales larger than the shoots is also important and Ω_E is generally less than unity.

In (1), $G(\theta)$ is determined not only by the leaf angle distribution but also by the angle distribution of foliage clumps at all scales when they exist [16]. In fact, the angle distribution of individual needles in a shoot becomes almost irrelevant to radiation interception when the shoot is dense and allows little light penetration. In this case $G(\theta) = G_E(\theta)$, where $G_E(\theta)$ includes the effects of the geometry of all foliage structures larger than the shoot. Since it is generally valid that $G_E(\theta) = G(\theta)$ for conifer stands, (1) and (2) can be combined to show that

$$\Omega = \Omega_E \frac{L_E}{L} = \Omega_E/\gamma_s \tag{3}$$

where $\gamma_s = L/L_E$, which can be measured from samples of shoots as the ratio of half the total needle area in a shoot to half the total shoot surface area. This equation separates the foliage clumping into two components, one at scales smaller than the shoot (γ_s) and one at scales larger than the shoot (Ω_E). To know the total foliage clumping index Ω, which allows the calculation of L from the measured gap fraction $P(\theta)$ (1), the remaining task is to resolve the value of Ω_E. The TRAC is designed to measure Ω_E by utilizing the canopy gap size information. The following two gap size analysis methods of CB92 and CC9x are outlined. They can be used to calculate Ω_E using the TRAC data.

A. Gap Size Accumulation Method (The F Approach)

This method is developed by CC9x. When the radiation sensor travels along a transect, it measures the width of sunflecks (the sunlit patches) on the transect. After considering the penumbra effect, the width of the canopy gaps casting the sunflecks on the transect can be calculated [10]. The calculated gaps can be sorted in ascending order according to their size and an accumulated gap size distribution $F(\lambda)$ can be formed (Fig. 1), where $F(\lambda)$ is the fraction of the transect occupied by gaps larger than or equal to λ. $F(\lambda) = 0$ for $\lambda > \lambda_1$ since no gaps are found to be greater than λ_1. $F(\lambda)$ increases as

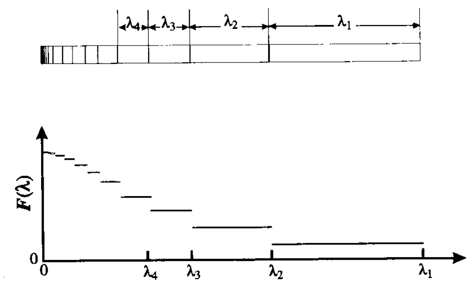

Fig. 1. Gap size accumulation from the largest to the smallest. The sectioned bar above shows gaps sorted in an ascending order from left to right according to the gap size.

λ decreases because of the contributions of smaller gaps. At $\lambda = 0$, $F(\lambda)$ becomes the total gap fraction of the canopy.

If foliage elements are random with respect to their spatial position, $F(\lambda)$ is given by (developed by CC9x after [17])

$$F(\lambda) = \left(1 + L_p \frac{\lambda}{W_{Ep}}\right) e^{-L_p(1+(\lambda/W_{Ep}))} \tag{4}$$

where

$$L_p = \frac{G(\theta) L_E}{\cos\theta} \tag{5}$$

and

$$W_{Ep} = \frac{\overline{W_E}}{\cos\theta_p}. \tag{6}$$

In the above equations, W_{Ep} is the mean width of the element shadows cast on the transect, and $\overline{W_E}$ is the mean width of an element projected on a plane perpendicular to the direction of the solar beam. The projected mean width depends on both the width and length of an element because the long axis of the element can be oriented at any angles relative to the transect direction. The term $1/\cos\theta$ compensates for the elongation of the element shadow on a horizontal plane in the direction of the transect, where θ_p is termed the "width projection angle." For elements with shapes which can be approximated by spheres, it is calculated as

$$\cos\theta_p = \sqrt{\frac{\cos^2\theta + \tan^2\Delta\beta}{1 + \tan^2\Delta\beta}} \tag{7}$$

where $\Delta\beta$ is the difference in the azimuthal angles of the sun and the transect. In this equation, θ_p varies from 0, at $\Delta\beta = \pi/2$, to θ, at $\Delta\beta = 0$ or π. For a canopy with a random spatial distribution of foliage elements, the gap size distribution will follow a $F(\lambda)$ curve defined by (4). In a clumped canopy, a measured accumulated gap size distribution denoted by $F_m(\lambda)$ deviates from $F(\lambda)$. When foliage elements are confined in structures such as branches and tree crowns, gaps between these structures appear. These gaps are generally larger than those in canopies without the structures. These large gaps appearing at probabilities greater than predicted for a random canopy with the same LAI and element width can be identified from the difference between $F_m(\lambda)$ and $F(\lambda)$. The contributions to the total gap fraction from these large gaps resulting from nonrandomness can therefore be removed by comparing $F_m(\lambda)$ with $F(\lambda)$. After the gap removal, a new distribution $F_{mr}(\lambda)$ is formed, which is $F_m(\lambda)$ brought to the closest agreement with $F(\lambda)$. In this case, $F_{mr}(0)$ is the total canopy gap fraction as if the canopy were random. The clumping index for foliage clumping at scales larger than the element (shoot) is therefore calculated as

$$\Omega_E = \frac{(1 + \Delta g)\ln[F_m(0)]}{\ln[F_{mr}(0)]} \tag{8}$$

where Δg is the total fraction of gaps removed.

In using $F(\lambda)$ as a basis for the gap removal, one must know L_E or L_p (5) and W_{Ep}. While W_{Ep} can be found from measurements of shoot samples, L_E or L_p is unknown because it is in fact the goal of finding Ω_E. CC9x solved the problem using an iterative method, which allows the simultaneous calculations of L_E and Ω_E. The first step in the iteration is to assume $L_p = -\ln[F_m(0)]$ and compute $F(\lambda)$ using (4). The measured gap size distribution $F_m(\lambda)$ is then compared with the first estimate of $F(\lambda)$. Since $F_m(\lambda)$ is always larger than $F(\lambda)$ at large λ values when a canopy is clumped, several largest gaps appearing at probabilities greater than $F(\lambda)$ are then removed. After the gap removal, a precursary $F_{mr}(\lambda)$ is thus formed. In the second step, L_p is taken to be $-\ln[F_{mr}(0)]$, which is smaller than the first estimate because the largest gaps have been removed in the first step. Using the new estimate of L_p, an improved $F(\lambda)$ is obtained and the same gap removal process as in the first step is iterated. The iteration continues until $F_{mr}(\lambda)$ is brought to the closest agreement with $F(\lambda)$, i.e., no significant increase in L_p is found in each step. Generally, L_p becomes asymptotic after 3–5 iterations. CC9x also developed a numerical method which finds the optimum value of W_{Ep} to be used in $F(\lambda)$ when the actual measurements of W_{Ep} are not available.

B. Gap Size Distribution Method (The P Approach)

Based on a theory developed in [17], CB92 used the following formula for describing the gap size distribution of a canopy with a random spatial distribution of foliage elements:

$$P(l) = \exp\left[-L_p\left(1 + \frac{l}{W_{Ep}}\right)\right] \tag{9}$$

where $P(l)$ is the probability of a probe of length l (with an infinitesimal thickness) falling completely within a sunfleck on the forest floor, or called the sunfleck (or gap) size distribution, L_p and W_{Ep} are defined in (5) and (6), respectively (for the convenience of notation, L_p is defined differently from that in CB92 where $\cos\theta$ is not included in L_p). This equation demonstrates that, under random conditions, $P(l)$ is determined by the total projected element area (L_p) in the sun's direction and the ratio of the probe length l to the characteristic width of the foliage elements (W_{Ep}). In this case, the distribution appears to be a straight line in a plot of $\ln P(l)$ versus l, where the slope of the line is determined by L_p/W_{Ep} (Fig. 2). For the same L_p, the slope decreases with increasing W_{Ep}.

When a canopy is clumped, the sunfleck size beneath the canopy is determined not only by the size of foliage elements

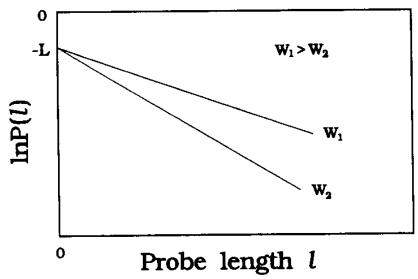

Fig. 2. Schematic gap size distributions for random plant canopies with the same leaf area index but different leaf sizes, where $W_1 > W_2$.

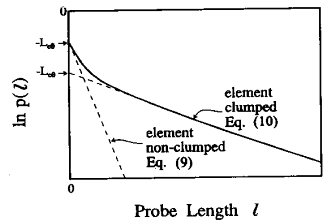

Fig. 3. A schematic gap size distribution for a clumped plant canopy, where $P(l)$ is a probability of an imaginary probe of length l falling completely within a sunfleck (sunlit patch) under the canopy. $P(0)$ is the total gap fraction which is only one point on the graph.

but also by the size of foliage clumps. CB92 found from measurements of sunfleck size distributions on the floor of a Douglas-fir stand that a large portion of the canopy gap size distribution can be explained by the presence of foliage clumps such as tree crowns. Under the assumptions of a random spatial distribution of foliage clumps and a random spatial distribution of foliage elements within each clump, they developed the following formula to determine $P(l)$ for clumped canopies:

$$P(l) = P_c(l) + P_{E1}(l)P_{c1} + P_{E2}(l)P_{c2} + \cdots = P_c(l) + \sum_{i=1}^{n} P_{Ei}(l)P_{ci} \quad (10)$$

where $P_c(l)$ is a sunfleck size distribution beneath a canopy with opaque clumps, P_{ci} is the probability of i number of clumps overlapping in the sun's direction, and P_{Ei} is a sunfleck size distribution within the intersection of i clumps. In this equation, i varies from 1 to n, where n can be infinite. This equation considers canopy gaps between clumps (the first term on the right-haand side (RHS)) and within a clump or clumps (the remaining terms). The terms are defined in the following equations:

$$P_c(l) = \exp[-L_{c\theta}(1 + l/W_{cp})] \quad (11)$$

$$P_{Ei}(l) = \exp[-iL_{Ep}(1 + l/W_{Ep})] \quad (12)$$

and

$$P_{ci} = \frac{\exp(-L_{c\theta}) \times L_{c\theta}^n}{i!} \quad (13)$$

where

$$L_{c\theta} = L_c/\cos\theta. \quad (14)$$

L_c is the projected clump area index. The projected clump area is defined as the area enclosed by the smoothed outline of a clump projected on a plane M perpendicular to the direction of projection. In (12), L_{Ep} is the sum of the individual element areas within a clump projected on M divided by the projected clump area.

The distribution of $P(l)$ predicted by (10) is shown in Fig. 3. At large l values, the distribution appears to be a straight line because the first term $P_c(l)$ dominates. If the clumps are opaque, the other terms in (10) are all zero, and the distribution will be a straight line at all values of l. The slope in this case will be determined by the clump area index and the clump size only. Since the foliage clumps, such as tree crowns, are not opaque, the curve turns upward as l decreases to values close to zero. This is because the small gaps within the clumps have contributions to the probability of small probes being exposed completely to the sun. In a plot like this, two intercepts on the ordinate can be found. One is the intercept of the curve, which is $L_{e\theta}$, or $-\ln P(0)$. The other, $L_{c\theta}$, is the intercept found from extrapolating the straight portion of the curve at large l values. These two intercepts determine the element clumping index Ω_E from

$$\Omega_E = \frac{L_{e\theta}}{L_{Ep}L_{c\theta}} \quad (15)$$

where L_{Ep} is calculated from $L_{e\theta}$ and $L_{c\theta}$ as follows (see (16), shown at the bottom of this page): In this equation, $\alpha = L_{c\theta}P_{E1}(0)/3$. This equation is derived from (10) after being truncated at $i = 2$. α compensates for the higher order terms. The truncation is made because in plant canopies the probability of observing gaps within the intersection of more than three clump overlappings is very small.

It may be noticed that although there are many definitions used in the theory, the determination of Ω_E is straightforward once a plot of $P(l)$ is obtained. When measurements of gaps λ_i, $i = 1, 2, 3, \cdots, m$, along transects beneath a canopy are available, $P(l)$ is calculated as

$$P(l) = \frac{1}{L_t}\sum_{i=1}^{m} u(\lambda_i - l)(\lambda_i - l) \quad (17)$$

where $u(x)$ is the unit step function defined as follows:

$$u(x) = \begin{cases} 1, & x > 0 \\ 0, & x \leq 0. \end{cases} \quad (18)$$

This unit step function is used to ensure that $(\lambda_i - l) = 0$ when $l \geq \lambda_i$, i.e., no probability of observing the probe l falling

$$L_{Ep} = \ln \frac{(1+\alpha)L_{c\theta}\exp(-L_{c\theta})}{\sqrt{2(1+\alpha)\exp[-(L_{e\theta} + L_{c\theta})] - (1+2\alpha)\exp(-2L_{c\theta})} - \exp(-L_{c\theta})}. \quad (16)$$

TABLE I
SITE DESCRIPTION

stand	age (year)	tree height (m)	density (stems/ha)	Latitude (deg)	Longitude (deg)	transect length (m)
NOJP	50-65	9-13.5	1300-2500	55.928 N	98.624 W	210
SOJP	60-75	12-15	500-1100	53.916 N	104.692 W	200
SYJP	11-16	4-5	4000-4100	53.877 N	104.647 W	150
SOBS	0-155	0-10	3700-4400	53.987 N	105.122 W	270

completely in λ_i when $l \geq \lambda_i$. To obtain $P(l)$ from $l = 0$ to $l \leq \lambda_{\max}$, where $\lambda_{\max}$ is the maximum gap size measured, (17) is repeatedly used with the same λ_i but different l.

One of the advantages of the P approach is its ability to determine the characteristic width of clumps (W_{cp}) from the slope of the straight portion of the curve at large l values and the characteristic width of foliage elements (W_{Ep}) from the slope of the tangent of the curve at $l = 0$.

III. Experimental Methods

Field measurements using the TRAC were made in August 1993 in four boreal conifer stands. The stand attributes are listed in Table I, where NOJP denotes an old jack pine (*Pinus banksiana*) stand in the northern boreal forest near Thompson, Manitoba, and SOJP, SYJP, and SOBS denote an old jack pine, a young jack, and an old black spruce (*Picea mariana*) stand, respectively, in the southern boreal forest near Candle Lake, Saskachewan. These stands are selected as the BOREAS tower flux sites. They are homogeneous at scales up to 1 km.

A transect was set up in each of the stands (Table I), extending southeast (±0.5°) from the flux tower. A forestry flag was inserted into the ground every 10 m along the transect to serve as a distance marker for the TRAC. The TRAC consists of a quantum sensor (LI-COR, Lincoln, NE, Model LI-190SB, 10-μs time constant) and a data logger (Campbell Scientific, Logan, UT, Model CR10) with a storage module with a capcity of 716 kb (Model SM716). The sensor is supported by a metal arm and the whole system is carried by a person walking along the transect. The data logger samples the voltage signal from the sensor at a rate of 32 Hz. If the walking speed is 0.33 m/s, then a sampling rate of 100 readings/m can be achieved. The walking speed was above 0.35 m/s and was not constant, resulting in a small range of measurement spacing from 10 to 13 mm. During measurements, a button on the supporting arm is pressed at each flag location along the transect and a pulse signal is sent to the data logger to register the distance. From the number of measurements in each 10-m interval between two pulses, the average spacing of the measurements is calculated.

On the same transects, measurements of the PCA were made every 10 m. The gap fractions from the PCA were larger by 12% on average than those from the TRAC at the same angle. For example, in SOJP at a solar zenith angle of 41.2°, the gap fraction from the TRAC was 0.29, while the PCA result at the same angle (interpolated between the available angles of 38° and 53°) was 0.33. The larger values from the PCA resulted from scattering of blue light in the canopy.

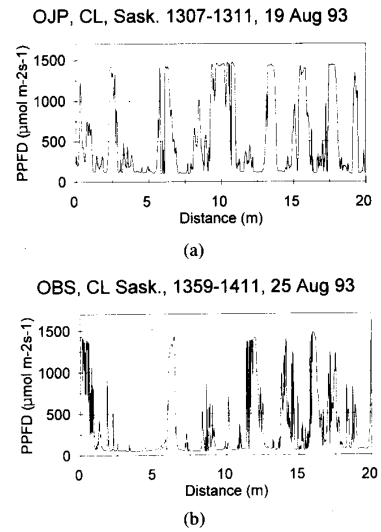

Fig. 4. Measurements of the photosynthetic photon flux density (PPFD) using the TRAC on transects in (a) an old jack pine stand (SOJP) at LDT 1307-1311 on Aug. 19, 1993 and (b) an old black spruce stand (SOBS) at LDT 1359–1411 on Aug. 25, 1993 near Candle Lake, Saskathewan. The spikes indicate sunflecks resulting from the penetration of direct light and the elevated baseline signifies the level of diffuse irradiance on the forest floor.

IV. Results

Portions (20 m) of the instantaneous photosynthetic photon flux density (PPFD) measured on the transects are shown as examples in Fig. 4 for SOJP and SOBS. The transmitted PPFD varies rapidly along the transects. The variations are characterized by large sunflecks (large blunt or flat-topped spikes) between tree crowns and small sunflecks (small sharp spikes) within tree crowns. In large sunflecks, the measured PPFD reaches the maximum value (P_{D+d}), which is treated as the sum of the direct PPFD above the canopy (P_D) and diffuse PPFD beneath the canopy (P_d). Since P_d forms a baseline in a plot of the total transmitted PPFD, P_D required in the calculation of canopy gap size is determined from the difference between the maximum value and the baseline. CB92 and CC9x developed a method to calculate the size of each canopy gap corresponding to each of the spikes, large or small, after considering the penumbra effect of the sun. The same method is used in this study.

Fig. 5 shows results from TRAC data processed using the F and P approaches. Fig. 5(a) shows the accumulated gap fraction $F_m(\lambda)$ as a function of canopy gap size λ. The length of the transect is 200 m. It can be seen from the measured distribution indicated by "Fm" that there are many gaps larger than 500 mm. The three largest gaps are 1.85, 1.78, and 1.5 m. If the foliage elements in the canopy were randomly positioned in the canopy, these large gaps resulting from the spaces between tree crowns would not have existed. Following the gap removal procedure of CC9x, gaps appearing at probabilities larger than predictions for a random canopy with the same element area index are removed from the total gap fraction accumulation. After the gap removal, a new distribution marked as "Fmr" is formed. The distribution for the random case denoted by "Fr" is determined from the

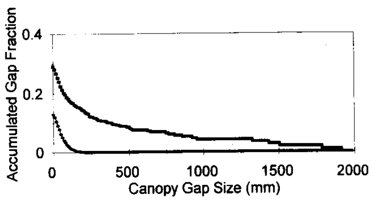

(a)

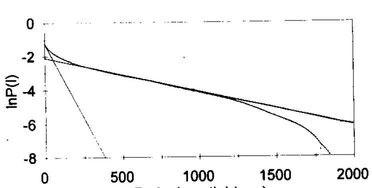

(b)

Fig. 5. (a) Gap size accumulation (F approach) and (b) gap size distribution (P approach) determined from sunfleck measurements at a solar zenith angle of 41.2° (LDT 1307-1311 on August 19, 1993) for an old jack pine stand (SOJP) near Candle Like, Manitoba.

new total gap fraction calculated to be 0.129 and the input of element size (60 mm). It almost completely overlaps with the Fmr distribution (Fig. 5(a)), indicating that an optimal adjustment of the accumulated gap fraction by gap removal has been achieved. It can be seen from the distributions of Fmr and Fr that all gaps larger than 200 mm would not have existed if the canopy were random. After the gap removal, the total canopy gap fraction was reduced from 0.289 to 0.129, i.e., in (8), $F_m(0) = 0.289, F_{mr}(0) = 0.129$, and $\Delta g = 0.16$, resulting in $\Omega_E = 0.70$.

Fig. 5(b) is calculated using the same data as Fig. 5(a). On the abscissa is the imaginary probe length, l, and on the ordinate is $P(l)$, the probability of the probe l being exposed completely to the sun calculated using (17). At $l = 0$, $P(l)$ is the canopy gap fraction, i.e., $P(0) = F_m(0)$. In this case, $\ln P(0) = \ln 0.29 = -1.24$, which is the intercept of the curve on the ordinate. The distribution of $\ln P(l)$ with l is not linear, indicating the spatial distribution of foliage elements is not random. However, for the values of l between 400 and 1200 mm, a linear portion of the curve exists. This portion of sunfleck size distribution results from gaps between foliage clumps. From the slope of the straight portion of the curve, which is 0.002 mm^{-1}, it can be determined that the average width of the clumps projected onto the transect is 1.1 m. This width is approximately the size of a tree crown, suggesting that tree crowns are the major foliage clumps. The curve drops off at large l values because the size of canopy gaps is always finite although the theory predicts very small probabilities for however large probe lengths. The effects of the 1.78-m gap (and other gaps about 1.5 m) on the distribution can be identified on the curve (slightly larger upward trend towards smaller l values). If the clumps were opaque, the curve would have remained straight down to $l = 0$. Since there are small gaps within the clumps (tree crowns), the curve inflects upwards as l decreases towards the intercept on the ordinate. The elevation of the measured curve at $l = 0$ above the extrapolated line from the linear portion of the curve allows the calculation of the foliage density of individual clumps. The effective leaf area index and the clump area index at the incidence angle θ, i.e., $L_{e\theta}$ and $L_{c\theta}$, are 1.24 and 2.19 from the interceptions, respectively. Using (16), the projected element area index within a clump L_{Ep} is calculated to be 0.82. The element clumping index Ω_E is then $1.24/(2.19 \times 0.82) = 0.69$ (15). This value agrees very well with that calculated from Fig. 5(a). From the slope of the tangent on the curve at $l = 0$, the width of the foliage elements is found to be 77 mm, which is slightly larger than 60 mm used for the shoots (see Fig. 9). This result supports the proposition that shoots in conifer stands are the basic foliage elements affecting radiation penetration into the canopy. Since needles in a shoot are tightly grouped together, the small gaps between needles are either nonexistent or disappear after a short distance due to the penumbra effect. CB92 also found that element size derived from a $\ln P(l)$ distribution is slightly larger than the characteristic width of shoots. This small discrepancy may have resulted from the inaccuracy of determining small canopy gaps from the apparent sunfleck width.

Fig. 6 shows similar results for NOJP. The length of the transect on which the TRAC measurements were made was 210 m. On that transect, the largest canopy gap was 1.01 m, the second largest 0.72 m, and numerous gaps larger than 0.2 m. After applying CC9x's procedure, almost all the gaps larger than 0.2 m are removed. After the gap removal, the distribution "Fmr" is formed, which in this case is slightly different from "Fr." In the calculation of Fr, W_{Ep} is assumed to be 50 mm. The total accumulated canopy gap fraction is reduced from 0.205 to 0.128. From these values, an element clumping index of 0.83 is calculated using (15). Fig. 6(b) shows the corresponding $\ln P(l)$ distribution, which is similar to that of Fig. 5(b). From the values of $L_{e\theta} = -\ln 0.205 = 1.58$ and $L_{c\theta} = 2.8$, the element clumping index Ω_E is calculated to be 0.71 ((16) and (15)). This value is 12% smaller than that derived using the F approach (Fig. 6(a)). From the slopes of the tangent at $l = 0$ and the straight portion of the curve in Fig. 6(b), it is determined that $W_{Ep} = 48$ mm and $W_{cp} = 0.54$ m. It is expected that the tree crown size is smaller than that of SOJP at a lower latitude. The effect of the second largest gap (0.72 m) on the distribution of $\ln P(l)$ can be more easily identified in this case.

Fig. 7 shows results for SYJP. There are many large gaps on the transect of 170 m, the four largest gaps being 1.89, 1.69, 1.62, and 1.43 m (Fig. 7(a)). The total accumulated gap fraction changes from 0.389 to 0.196 after the gap removal calculated with $W_{Ep} = 40$ mm, thus yeilding $\Omega_E = 0.69$. In Fig. 7(b), it can be determined that $L_{e\theta} = 0.94$ and $L_{c\theta} = 1.85$. From these values, therefore $\Omega_E = 0.73$ ((16) and (15)). The widths of the elements and clumps calculated from the slopes are 49 mm and 0.95 m, respectively.

Fig. 8 shows results for SOBS. The total transect length is 270 m, and the largest gap is 0.95 m. There are many medium-sized gaps around 0.5 m. Applying the gap removal procedure of CC9x to the data set with $W_{Ep} = 30$ mm results in a change in the total gap fraction from 0.190 to 0.103. From this

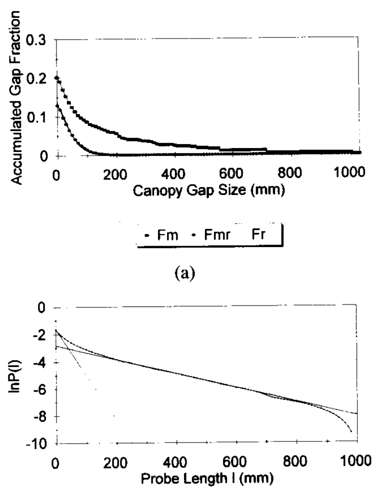

Fig. 6. (a) Gap size accumulation (F approach) and (b) gap size distribution (P approach) determined at a solar zenith angle of 60.1° (LDT 1721-1728 on August 16, 1993) for an old jack pine stand (NOJP) near Thompson, MB, Canada.

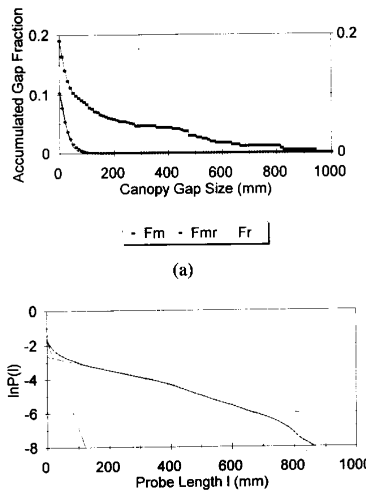

Fig. 8. (a) Gap size accumulation (F approach) and (b) gap size distribution (P approach) determined at a solar zenith angle of 44.8° (LDT 1340-1410 on August 25, 1993) for an old black spruce stand (SOJP) near Candle Lake, Saskathewan.

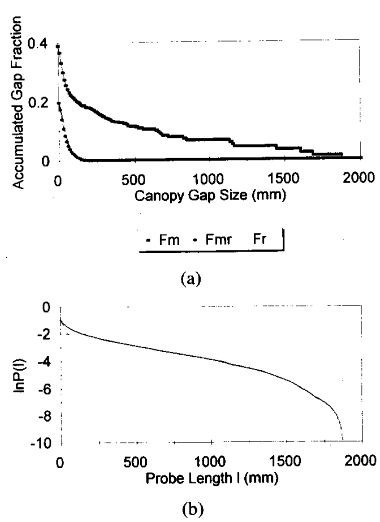

Fig. 7. (a) Gap size accumulation (F approach) and (b) gap size distribution (P approach) determined at a solar zenith angle of 41.8° (LDT 1257-1302 on 21 August 1993) for a young jack pine stand (SYJP) near Candle Lake, Saskathewan.

change, it is computed that $\Omega_E = 0.79$. In the corresponding $\ln P(l)$ distribution, it is determined that $L_{e\theta} = 1.64$ and $L_{c\theta} = 2.75$, and therefore $\Omega_E = 0.68$. It is also determined from Fig. 8(b) that $W_{Ep} = 32$ mm and $W_{cp} = 0.70$ m. It is noted that the linear portion of the curve in Fig. 8(b) is small, and therefore the determination of the slope and $L_{c\theta}$ may not be accurate in this case. This also affects the accuracy of Ω_E. The drop of the curve from the expected straight line at about $l = 400$ mm (Fig. 8(b)) is due to the large decrease in the accumulated gap fraction as the gap size increases from 400 to 600 mm (Fig. 8a). The abnormal distribution in $\ln P(l)$ when the random assumption is not satisfied causes uncertainties in the derived parameters. On the contrary, the detailed $F_m(\lambda)$ distribution at large λ does not affect the calculated Ω_E. This suggests that the F approach is generally more robust than the P approach.

Fig. 9 is shown for the purpose of evaluating the effect of the choice of the element characteristic width W_E on the computed value of Ω_E, since W_E is a critical input in using the F approach. In the figure, each curve represents the average for a stand. In all four cases, the element clumping index increases with increasing element width. The increase is steep at small element widths but becomes asymptotic as the width increases. CC9x found that the increase in Ω_E begins to level off at W_E values close to the characteristic widths of shoots, 59 and 130 mm for a jack pine and a red pine stand, respectively. The cases shown here are similar: the curves begin to increase much slower at about W_E = 30, 40, 50, and 60 mm for the SOBS, SYJP, NOJP, SOJP stands, respectively. The shoots in these jack pine stands are similar in shape and size to those in the jack pine stand investigated by CC9x. Shoots in black spruce stand studied here are considerably smaller than those of jack pine and are estimated to have a characteristic width of 30 mm. If the size of the elements is uniform, little increase in Ω_E is expected at input W_E values larger than the actual W_E. The gentle increases shown in Fig. 9 indicate that the element size in each of the canopies may not be uniform and foliage structures larger than the shoots, such as subbranches, branches, and branch clusters, have effects on the gap size accumulation. In theory, the effects of structures larger than the elements (shoots) are eliminated in the gap removal processes with only gaps expected for a canopy with a random distribution of elements being retained. However, some of these effects may remain when small gaps between elements are not accurately measured. This appears to be the only major source of error in the F approach.

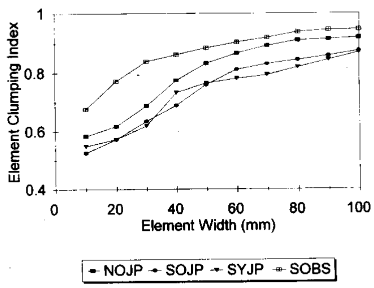

Fig. 9. Computed element (shoot) clumping index Ω_E as affected by the input values for the projected element characteristic width W_{Ep} for all for stands investigated.

Key variables and the main results for all the stands are given in Table II. For the element clumping index Ω_E, (P) and (F) indicates results from the P approach and the F approach, respectively. W_{Ep} and W_{cp} are the projected element and projected clump characteristic widths derived using the P approach. The Ω_E values from the F approach were calculated with W_{Ep} given to be 30, 40, 50, and 60 mm for the SOBS, SYJP, NOJP, and SOJP, respectively. These widths are determined from Fig. 9 as the points at which the curves begin to level off, with an error of less than ± 10 mm. W_{Ep} is larger than W_E by a small amount depending on the solar zenith angle and the difference between azimuth angles of the sun and the transect. Two numbers in Table II are marked with "*" because they are not meaningful. The first one, 106 mm, for the element size in the NOJP stand is unrealistically large (the size of the shoots is estimated to be about 50 mm). The problem is caused by the low solar elevation (large zenith angle of 67.4°) at which the solar illumination is low and the penumbra effect becomes serious. The penumbra effect makes it difficult to delineate small sunflecks when the distance from the foliage to the forest floor is large. This indicates that both gap size analysis methods suffer from the limitation in our ability to detect small canopy gaps using optical sensors at low solar elevations. The range of solar zenith angle in which small canopy gaps (about 5 mm) can be detected is found to be from 0 to 60°. Therefore, it is suggested that sunfleck measurements for characterizing the canopy architecture be made within this range. When small gaps are not detected, the slope of the tangent of the $\ln P(l)$ curve at $l = 0$ decreases and the value of the element size, which is inversely proportional to the slope, increases. This explains the reason for the unrealistically large value of 106 mm for the element size for this transect measurement.

The second unrealistic value marked with "*" is 2.1 m for the clump size in the SYJP stand. This value is derived because two gaps larger than 2 m were measured on a transect of about 110 m. These two gaps reduce the slope of $\ln P(l)$ at large l values and therefore increase the clump size which is inversely proportional to the slope. This error exists because of the assumption of random spatial distribution of foliage clumps used in deriving the theory for the P approach. Although this assumption is generally valid for natural forests, it may be violated seriously in some cases. This abnormal case appears because 1) this transect is shorter than the others (170 m),

TABLE II
SUMMARY OF VARIABLES AND RESULTS (LDT: LOCAL DAYLIGHT-SAVING TIME, BEING GREENWICH MEAN TIME (GMT)—6 h FOR SASKACHEWAN AND GMT—5 h FOR MANITOBA)

site	day num.	time (LDT)	β_t (deg)	β_s (deg)	$\Delta\beta$ (deg)	θ_s (deg)	Ω_E (P)	Ω_E (F)	W_{Ep} (mm)	W_{cp} (m)
NOJP	228	1733-1738	135	251.3	116.3	61.5	0.74	0.83	48	0.54
NOJP	228	1817-1819	135	260.9	125.9	67.4	0.59	0.83	106*	0.66
SOJP	231	1307-1311	135	182.4	47.4	41.2	0.69	0.70	77	1.10
SOJP	231	1531-1543	135	231.1	96.1	51.0	0.73	0.85	59	0.83
SOJP	231	1727-1734	135	258.7	123.7	66.1	0.62	0.89	55	0.45
SYJP	233	1257-1302	135	179.3	44.3	41.8	0.73	0.69	49	0.95
SYJP	233	1348-1252	135	197.4	62.1	42.5	0.74	0.71	50	2.1*
SYJP	233	1600-1604	135	237.9	104.9	54.4	0.60	0.80	42	0.51
SOBS	237	1359-1411	135	201.6	67.6	44.8	0.68	0.79	32	0.70
SOBS	237	1653-1700	135	250.3	115.3	63.3	0.78	0.89	36	0.52

and 2) the SYJP stand is characterized by clumps of trees. A practical solution to this problem is to increase the length of the transect. When the assumption is not met, a considerable error is also expected in the derived Ω_E value using the P approach. However, in the F approach, such an assumption is not required. Therefore, the F approach is free from the error resulting from different spatial distribution patterns of foliage clumps. If a transect runs through a large opening in a stand, for example, the effect of this large gap can be entirely eliminated in the F approach because this excessively large gap will be identified in an $F_m(\lambda)$ distribution and eliminated after applying the gap removal procedure. Because of this flexibility, the F approach can be used for all types of vegetation covers including heterogeneous canopies.

It is also interesting to note in Table II that as the solar zenith angle (θ_s) increases, W_{cp} decreases in most of the stands (SYJP, SOJP, and SOBS). This trend of variation may result from the fact that conifer tree crowns largely consist of horizontal branches and break down into branches when viewed from near the horizontal direction. Similar results were found by CB92 for a Douglas-fir stand. The corresponding values of Ω_E from the F approach show increasing trends with increasing θ_s, suggesting that as tree crowns gradually break down into branches at high solar zenith angles the canopies became less clumped. These findings indicate that for modeling radiation in conifer canopies, the scales of foliage structure to be considered should at least include tree crowns, branches, and shoots.

Fig. 10 compares Ω_E values derived using the F and P approaches for the four stands investigated. On average, the values from the F approach are about 10% larger than those from the P approach. The reason for the systematic discrepancy may be that the computation of Ω_E is negatively biased using the P approach by the assumption of a random spatial distribution of foliage clumps. Under this assumption, there are probabilities for clumps (tree crowns) to overlap, whereas in nature this situation rarely happens because tree crowns are more or less at the same height. In reality, the shadow of one tree crown only overlaps with the lower portions of other tree crowns in the downward direction of the penetrating light, and the probability of tree crown shadow overlapping in the sun's direction is smaller than

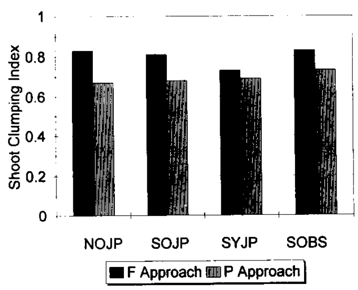

Fig. 10. Comparison between the results of element clumping index Ω_E calculated using the F and P approaches.

that predicted under the randomness assumption. Also, the natural repulsion effect, which inhibits the growth of trees in close proximity to other trees, eliminates the probability of one tree crown being merged in depth with another. This makes the probability of tree crown overlapping smaller than that predicted by the Poisson theory. An overlapping probability smaller than assumed means less clumping of foliage than calculated. This may explain the reason for the smaller values of Ω_E (more clumped) derived using the P approach than those from the F approach. We believe that the values from the F approach are more reliable since no assumptions for the spatial distribution patterns of foliage elements and clumps are made in establishing the F approach. However, both approaches share the same error resulting from the inaccuracy in determining very small canopy gaps from sunfleck measurements. Since the radiation sensor has a very small time constant (10 μs), its traveling speed does not affect the measurements. The inaccuracy in measuring the very small gaps is due to the penumbra effect. We found that the error is less than 3% in Ω_E for transect measurements made at solar zenith angles smaller than 60°. According to the results of the F approach, it appears that the effect of foliage clumping, at scales larger than shoots, on optical measurements of leaf area index is about 15–25% for all the boreal stands investigated.

V. Discussion

The Ω_E results from the P approach suffer from a considerable error due to the assumption of a random distribution of foliage clumps. However, this approach is still useful in deriving the canopy architectural parameters L_c, L_E, L_{Ep}, W_c, and W_E. This study confirms the finding of CB92 that W_E derived from the slope of the tangent on the curve of $\ln P(l)$ at $l = 0$ is approximately equal to the characteristic width of shoots in conifer stands. The curve pattern shown in Fig. 9 also provides confirmation to this finding. This architectural information is important in optical measurements of LAI of conifer canopies because it suggests that the amount of overlapping of needles within individual shoots cannot be detected from the light penetration measurements. In this case, destructive sampling of shoots is necessary to determine the effect of within-shoot needle clumping on optical measurements of LAI.

Stimulated by the need to describe the directional reflection behavior of vegetated surfaces in remote sensing applications, increasing research attention has been given to modeling radiation transfer processes within plant canopies. After Li and Strahler [18], in which conifer canopies are assumed to consist of solid cones, considerable research has been directed toward modeling more realistic canopies with nonopaque tree crowns [19]–[23]. To model the different components of a forested surface, such as sunlit and shaded tree crowns and shadows on the ground surface as seen from a particular view angle relative to the solar illumination angle, it is important to know the probability of light penetration through the tree crowns. The parameter L_{Ep} derived from the P approach characterizes the average amount of foliage to intercept a beam of light through a tree crown in the direction of light and therefore can be used to calculate the penetrability of the tree crown in the same direction. The other parameters of L_c, L_E, and W_c are also useful in models of this type. In Fig. 4, for example, $L_{c\theta}$ and $L_{e\theta}$ are found from the intercepts to be 2.19 and 1.24, respectively. This means that the total canopy gap fraction (or the percent ground surface which can be seen along the direction of a solar beam) is $e^{-1.24} = 0.29$ and the gap fraction resulting from the spaces between clumps (tree crowns) is $e^{-2.19} = 0.11$. The contribution of the gaps within tree crowns to the total gap fraction is then $0.29 - 0.11 = 0.18$. The contribution in this case is more than 60% of total gap fraction. This simple calculation using the results from the P approach suggests that the gaps within tree crowns are important in determining radiation transfer regimes in the canopy. However, this calculation is in error when the assumptions in the P approach are not satisfied. Our further research will be directed toward combining the F and P approaches to derive more accurate canopy architectural parameters.

In addition to measuring LAI, the TRAC also provides continuous transect measurements of the total sunlight penetrating the forest canopy, which is essential to obtain the mean PPFD beneath the overstory. From the total PPFD, the direct and diffuse components can be separated. These measurements are useful for micrometeorological and ecological studies and for validating radiative transfer models.

VI. Conclusions

The new optical instrument, named the TRAC, was successfully used to measure the effect of canopy architecture on indirect measurements of leaf area index of boreal conifer canopies. Two gap size analysis methods are used to calculate the element clumping index (Ω_E) quantifying the effect of foliage clumping at scales larger than the element (shoot). One of them is the gap size accumulation method (the F approach) of CC9x and the other is the gap size distribution method (the P approach) of CB92. The values of Ω_E derived using these two approaches agree within 5–17%, with P approach values consistently smaller than F approach values. Ω_E values from the P approach are negatively biased because of the assumption of a random spatial distribution of foliage clumps. The F approach is superior because it requires no such assumption. Reliable canopy architectural information can be obtained at solar zenith angle smaller than 60°.

According to the results derived using the F approach, the effect of foliage clumping at scales larger than the shoots reduces the optical measurements of LAI based on canopy gap fraction by a factor of about 15–25% for boreal forest stands. The results from both the P and F approaches confirm the validity of the generally accepted assumption that needle shoots in conifer stands are the basic foliage units responsible for radiation interception. This suggests that an additional step is required to measure the amount of needle area within individual shoots before the effect of all levels of foliage clumping can be quantified.

The element clumping index can be used as a correction of LAI measurements made using the LI-COR LAI-2000. Optical measurements of LAI made with a combination of the LAI-2000 and the TRAC can be more accurate than partial direct measurements through destructive sampling.

VII. List of Symbols

c	shape factor (ratio of W to w)
Δg	total fraction of gaps
$G(\theta)$	projection of unit leaf area on M
$G_E(\theta)$	projection of unit element (shoot) area on M
l	imaginary probe length
L	plant area index or leaf area index when woody materials are ignored
L_c	clump area index projected on M
$L_{c\theta}$	$= L_c/\cos\theta$
L_e	effective leaf area index as measured by the PCA, being ΩL
$L_{e\theta}$	$= L_e/\cos\theta$
L_E	element (shoot) area index
L_{Ep}	sum of the individual element area within a clump projected on M divided by the area enclosed by the smoothed outline of the clump projected on M
L_p	projected element area index
L_t	length of measurement transect
M	plane perpendicular to the solar beam
w	maximum element width in the transect direction
W_E	characteristic element width
W_{Ep}	element width projected on a horizontal surface in the transect direction
W_c	characteristic clump width
W_{cp}	clump width projected on a horizontal surface in the transect direction
$F(\lambda)$	accumulated canopy gap size distribution for a random distribution of the spatial position of foliage elements
$F_m(\lambda)$	measured canopy gap size distribution
$F_{mr}(\lambda)$	measured canopy gap size distribution after processing to resemble $F(\lambda)$
$P(l)$	probability of a probe l being completely exposed to the sun
$P_c(l)$	$P(l)$ for a canopy composed of opaque clumps
$P_E(l)$	$P(l)$ within smoothed boundary of a clump
$\Delta\beta$	difference between azimuth angles of the sun and the transect
β_t	azimuthal angle of the transect
γ_E	ratio of half the total leaf (needle) area in a shoot to half the total shoot area, being equal to L/L_E
λ	canopy gap size
θ	solar zenith angle
θ_p	width projection angle depending on θ and $\Delta\beta$
ρ	number of foliage elements per unit ground surface area
σ	foliage element area
Ω	clumping index for leaves (needles)
Ω_E	clumping index for elements (shoots)

Acknowledgment

M. Xie of CCRS assisted in the field data collection. G. Fedoseyevs of CCRS carefully reviewed the manuscript before it was submitted to this journal.

References

[1] J. M. Welles, "Some indirect methods of estimating canopy structure," in N. S. Geol and J. M. Norman, Eds., *Instrumentation for Studying Vegetation Canopies for Remote Sensing in Optical and Thermal Infrared Regions. Remote Sensing Rev.*, vol. 5, pp. 1–12, 1990.

[2] G. D. Badhwar, R. B. MacDonald, and N. C. Mehta, "Satellite-derived leaf-area-index and vegetation maps as input to global carbon cycle models—A hierarchical approach," *Int. J. Remote Sensing*, vol. 7, pp. 265–281, 1986.

[3] D. L. Peterson, M. A. Spanner, S. W. Running, and K. B. Teuber, "Relationship of Thematic Mapper simulator data to leaf area index of temperate coniferous forest," *Remote Sensing Environ.*, vol. 22, pp. 323-341, 1987.

[4] M. A. Spanner, L. L. Pierce, D. L. Peterson, and S. W. Running, "Remote sensing temperate coniferous forest leaf area index. The influence of canopy closure, understory and background reflectance," *Int. J. Remote Sensing*, vol. 11, no. 1, pp. 95–111, 1990.

[5] ——, "The seasonal trends of AVHRR data of temperate coniferous forests: Relationship with leaf area index," *Remote Sensing Environ.*, vol. 33, pp. 97–112, 1990.

[6] M. A. Spanner, L. Johnson, J. Miller, R. McCreight, J. Freemantle, J. Runyon, and P. Gong, "Remote sensing of seasonal leaf area index across the Oregon transect," *Ecol. Applic.*, vol. 4, pp. 258–271, 1994.

[7] J. M. Chen, T. A. Black, and R. S. Adams, "Evaluation of hemispherical photography for determining plant area index and geometry of a forest stand," *Agric. For. Meteorol.*, vol. 56, pp. 129–143, 1991.

[8] S. T. Gower and J. M. Norman, "Rapid estimation of leaf area index in forests using the LI-COR LAI-2000," *Ecology*, vol. 72, pp. 1896–1900, 1990.

[9] J. M. Chen and T. A. Black, "Foliage area and architecture of plant canopies from sunfleck size distributions," *Agric. For. Meteorol.*, vol. 60, pp. 249–266, 1992.

[10] J. M. Chen and J. Cihlar, "A gap size analysis theory for improving optical measurements of leaf area index of plant canopies," *Appl. Opt.*, in press.

[11] T. Nilson, "A theoretical analysis of the frequency of gaps in plant stands," *Agric. Meteorol.*, vol. 8, pp. 25–38, 1971.

[12] J. M. Chen and T. A. Black, "Defining leaf area index for non-flat leaves," *Plant, Cell Environ.*, vol. 15, pp. 421–429, 1992.

[13] G. Deblonde, M. Penner, and A. Royer, "Measuring leaf area index with the LI-COR LAI-2000 in pine stands," *Ecology*, vol. 75, pp. 1057–1511, 1994.

[14] K. Fassnacht, S. T. Gower, J. M. Norman, and R. E. McMurtrie, "A comparison of optical and direct methods for estimating foliage surface area index in forests," *Agric. For. Meteorol.*, vol. 71, pp. 183–207, 1994.

[15] P. Oker-Blom and S. Kellomaki, "The ratio of shoot silhouette area to total needle area in Scots pine," *For. Sci.*, vol. 34, pp. 894–906, 1998.

[16] J. M. Chen and T. A. Black, "Measuring leaf area index of plant canopies with branch architecture," *Agric. For. Meteorol.*, vol. 57, pp. 1–12, 1991.

[17] E. E. Miller and J. M. Norman, "A sunfleck theory for plant canopies. I. Lengths of sunlit segments along a transect," *Agron. J*, vol. 63, pp. 735–738, 1971.

[18] X. Li and A. H. Strahler,"Geometric-optical modeling of a conifer forest canopy," *IEEE Trans. Geosci. Remote Sensing*, vol. GRS-23, pp. 705–721, 1985.
[19] ——, "Gap frequency in discontinuous canopies," *IEEE Trans. Geosci. Remote Sensing*, vol. 26, pp. 161–170, 1988.
[20] ——, "Geometric-optical bidirectional reflectance modeling of mutual shadowing effects of crowns in a forest canopy," *IEEE Trans. Geosci. Remote Sensing*, vol. 30, pp. 276–292, 1992.
[21] N. S. Geol, I. Rosehnal, and R. L. Thompson, "A computer graphics based model for scattering from objects of arbitrary shapes in the optical region," *Remote Sens. Environ.*, vol. 36, pp. 73–104, 1991.
[22] R. B. Myneni, G. Asrar, and F. G. Hall, "A three-dimensional radiative transfer method for optical remote sensing of vegetated land surfaces," *Remote Sensing Environ.*, vol. 41, pp. 105–121, 1992.
[23] J. Ross and A. Marshak, "Monte Carlo methods," in *Photon-Vegetation Interactions*, R. B. Myneni and J. Ross, Eds. New York: Springer-Verlag.

Jing M. Chen received the B.Sc. degree in 1982 from Nanjing Institute of Meteorology, Nanjing, P. R. China, and the Ph.D. degree in 1986 from the University of Reading, Reading, UK.

He is currently a Research Scientist at the Canada Centre for Remote Sensing (CCRS) and an Adjunct Professor at the University of Ottawa, both in Ottawa, Ont., Canada. His main research interests have been in turbulent and radiative transfer processes associated with plant canopies. His current research is directed towards developing algorithms for deriving biophysical parameters of the earth's surface using satellite data and modeling boreal ecosystems.

Josef Cihlar (M'86–SM'88) received the B.Sc. Agr. degree in agricultural engineering, the M.Sc. degree in soil science, and the Ph.D. degree in geography and remote sensing.

Between 1975 and 1991, he worked as a Scientist and Head of the Applications Development Section at the Canada Centre for Remote Sensing (CCRS), Ottawa, Ont. Presently, he is a Research Scientist and Head of the CCRS Global Monitoring Section. His research interests focus on the use of satellite observations for monitoring and modeling environmental change over land at regional to continental scales. He is involved in several interdisciplinary projects, including the BOREAL Ecosystem-Atmosphere Study (BOREAS) and the Northern Biosphere Observation Modeling Experiment (NBIOME).